Enhancement of antibacterial properties of Ag nanorods by electric field

To cite this article: Omid Akhavan and Elham Ghaderi 2009 *Sci. Technol. Adv. Mater*. **10** 015003

View the article online for updates and enhancements.

Enhancement of antibacterial properties of Ag nanorods by electric field

Omid Akhavan[1] and Elham Ghaderi[2]

[1] Department of Physics, Sharif University of Technology, PO Box 11155-9161, Tehran, Iran
[2] Tehran University of Medical Sciences, PO Box 14155-6447, Tehran, Iran

E-mail: oakhavan@sharif.edu

Abstract

The effect of an electric field on the antibacterial activity of columnar aligned silver nanorods was investigated. Silver nanorods with a polygonal cross section, a width of 20–60 nm and a length of 260–550 nm, were grown on a titanium interlayer by applying an electric field perpendicular to the surface of a Ag/Ti/Si(100) thin film during its heat treatment at 700 °C in an Ar+H_2 environment. The optical absorption spectrum of the silver nanorods exhibited two peaks at wavelengths of 350 and 395 nm corresponding to the main surface plasmon resonance bands of the one-dimensional silver nanostructures. It was found that the silver nanorods with an fcc structure were bounded mainly by {100} facets. The antibacterial activity of the silver nanorods against *Escherichia coli* bacteria was evaluated at various electric fields applied in the direction of the nanorods without any electrical connection between the nanorods and the capacitor plates producing the electric field. Increasing the electric field from 0 to 50 V cm^{-1} resulted in an exponential increase in the relative rate of reduction of the bacteria from 3.9×10^{-2} to 10.5×10^{-2} min^{-1}. This indicates that the antibacterial activity of silver nanorods can be enhanced by applying an electric field, for application in medical and food-preserving fields.

Keywords: antibacterial, silver, nanorods, Ti thin film

(Some figures in this article are in colour only in the electronic version)

1. Introduction

Metallic nanostructured materials [1], owing to their novel and unique size-dependent properties, have attracted much attention in antibacterial and biomedical [2–4], catalytic [5–8], optical [9, 10], electronic [11, 12] and quantum-size-domain [13] applications.

Silver has long been known as an inorganic material having strong inhibitory and bactericidal effects as well as antimicrobial activity against a broad range of microbes [14, 15]. Recently, systematic studies have reconfirmed the effective antimicrobial activity of silver [16–21]. In this regard, researchers strongly desire to renew the bactericidal application of silver, because of the evolution of new strains of bacteria that are resistant to current antibiotics [22].

It is generally believed that when Ag atoms transform into ions, the multiplication of bacteria may be prevented, probably because of the interaction of the ions with the DNA structure of bacteria [23, 24]. Furthermore, these positively charged ions may bind to the bacterial cell wall membrane (slightly negative), damage it and thus alter its functionality [23–25].

On the basis of this mechanism, silver can inhibit the growth of a wide variety of microorganisms such as molds, viruses, bacteria and so forth [26–30]. More importantly, silver nanostructures, such as silver nanoparticles, provide a large surface-area-to-volume ratio and a high fraction of surface atoms [31], which enhance the antimicrobial activity of silver, even at low concentrations [32–37]. The antibacterial action of electrodes [38], particularly silver electrodes, as

an extremely bacteriostatic material [39–41] when used as the anode, even at low currents, is also well known. Therefore, the development of silver nanostructure-based technology can promote the resurgence of the medical use of silver, particularly in applications designed to kill pathogen microorganisms.

In this work, we have studied a method in which an electric field was applied in the direction of silver nanorods grown on a titanium interlayer to enhance their antibacterial activity against *Escherichia coli* (*E. coli*) bacteria as a typical Gram-negative bacterium. In addition, the physical characteristics of the grown nanorods including surface topography, crystalline structure and optical properties were also investited.

2. Experimental details

2.1. Preparation of samples

P-type Si(100) wafers with a resistivity of 8–10 Ω cm and cut into 10×10 mm^2 pieces were used as substrates and cleaned by the standard Radio Corporation of America (RCA) method. This cleaning procedure is the industry standard method for removing contaminants from wafers, the basic procedure of which was developed by Werner Kern in 1965 while working for RCA. The native oxide on the surface of the substrates was subsequently removed by rinsing them in dilute HF solution (HF: $H_2O = 1 : 20$ by volume) for 20 s. Then, the wafers were dried by ultrahigh-purity nitrogen before loading into a vacuum chamber with a base pressure of about 2×10^{-6} Torr.

In each run, the deposition of a 10 nm Ti buffer layer was followed by that of a 100 nm Ag film by dc magnetron sputtering without breaking the vacuum. All depositions were performed in Ar discharge gas with a pressure of 5 mTorr. The film thicknesses were monitored *in situ* using a quartz crystal oscillator calibrated by the interferential optical technique.

The deposited samples were annealed at a high temperature of 700 °C in $Ar(80\%) + H_2(20\%)$ ambient with a flow rate of 1 litre min^{-1} for 30 min. During the heat treatment of the Ag/Ti/Si multilayer thin films, a uniform electric field (E_h) of 10 V cm^{-1} was applied normal to the thin film/substrate surface to control the growth of silver nanorods in one dimension. Note that no direct voltage was applied to the nanostructures, which were located between two plates of a capacitor producing the desired electric field, so that the polarity of the nanorod tips was positive.

2.2. Characterization of samples

Scanning electron microscopy (SEM) and atomic force microscopy (AFM) were utilized to study the surface topography of the grown nanostructures. A UV-visible spectrophotometer was used to determine the optical reflection and thus the absorption of the films containing silver nanorods in the wavelength range of 300–1100 nm with 1 nm resolution. Phase formation and the preferential crystallographic orientation of the samples were determined by θ–2θ x-ray diffraction (XRD) analysis from 15 to 85° with a step of 0.005 using radiation from a Cu-Kα source.

2.3. Antibacterial test

To evaluate the antibacterial activity of the grown silver nanorods, *E. coli* (American Type Culture Collection No. 25922) was selected as a typical Gram-negative bacterium. Before the microbiological experiment, all glassware and samples were sterilized by autoclaving at 120 °C for 15 min. The Ag nanorods grown on the Ti interlayer were immersed in 10 ml nutrient broth inoculated with about 10^5 cfu ml^{-1} *E. coli* (cfu = colony forming units). Then, the solution containing the sample was incubated in the dark in a shaking incubator at 37 °C for 50–135 min (depending on the antibacterial activity of the sample at different values of applied electric field). During the incubation process, an electric field (*E*) with a value in the range 10–50 V cm^{-1} was applied perpendicular to the film surface (parallel to the nanorods). For easy and accurate counting of the numbers of grown bacterial colonies, 0.1 ml of the treated solution was diluted with deionized water to a suitable volume. Then, the diluted solution was spread on a nutrient agar plate and incubated at 37 °C for 48 h before counting the number of bacterial colonies.

3. Results and discussion

Figure 1(a) shows an SEM image of a Ag/Ti/Si thin film heat treated at 700 °C without applying an electric field during the heat-treatment process. Many silver nanoparticles with a nearly cubic shape were formed among the heat-treated silver layer. The side length of the silver nanocubes was measured to be in the range of 15–50 nm. AFM analysis (not shown here) indicated that the average side length and height of the cubic nanoparticles were in the ranges of 40–70 and 30–90 nm, respectively. It can also be seen that the corners of the nanocubes were slightly truncated; thus, the silver nanoparticles formed mainly had a polygonal cross section. By applying an electric field perpendicular to the surface during the heat-treatment process, silver nanorods with a columnar structure and a polygonal cross section were produced on the Ti layer. Figure 1(b) shows a cross-sectional SEM image of the silver nanorods grown in an applied electric field on the Ti interlayer. The width and height of the nanorods are 20–60 and 260–550 nm, respectively. The Ti interlayer with a thickness of about 20 nm deposited on the Si substrate is also distinguishable in the SEM image. The thinner Ti layer compared with the as-deposited value may be related to the interdiffusion of Si and Ti atoms at their interface. It was previously shown that silver thin films with thickness $\geqslant$25 nm deposited on a Ti buffer layer retain their integrity at a high annealing temperature of 700 °C [42]. The aspect ratio of the tips of the silver nanorods (defined as the ratio of the height of the pyramidal tip to its width) was estimated as 0.4–0.7, corresponding to apex angles of 51–35°. Note that the formation of silver nanoparticles, nanowires and nanorods with polygonal cross sections has also been reported elsewhere (see for example, [43–45]).

Figure 2 shows the UV-vis absorption spectrum of the silver nanorods grown on the Ti interlayer. Two absorption bands located at about 350 and 395 nm characterize the
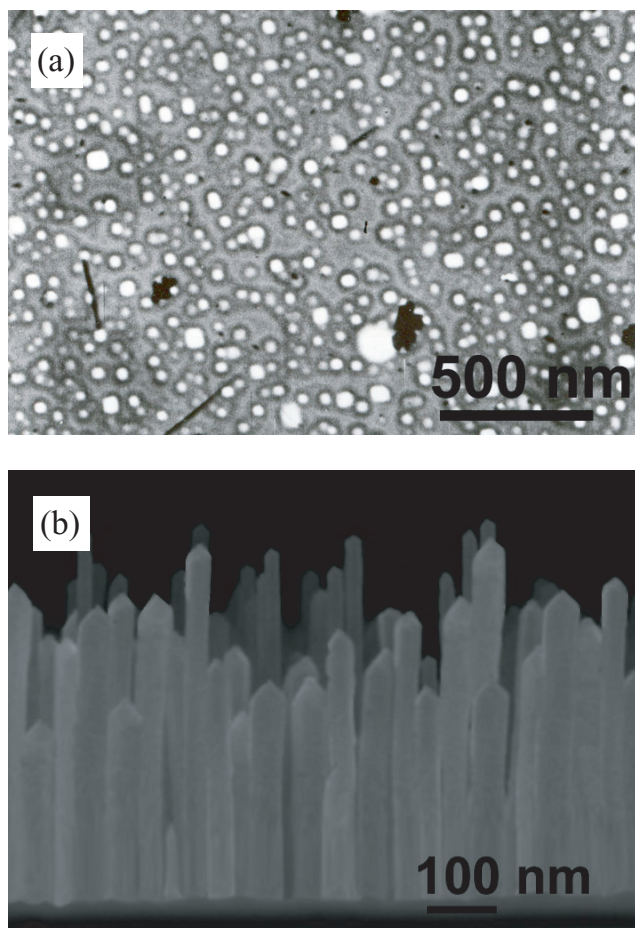
Figure 2. Optical density spectrum of the silver nanorods grown on a Ti interlayer.

Figure 1. (a) Top-view SEM image of the cubic silver nanoparticles grown on a Ti interlayer without the application of an electric field and (b) cross-sectional SEM image of the silver nanorods grown on a Ti interlayer while applying an electric field during the heat treatment.

spectrum. The peaks are attributed to the surface plasmon resonance (SPR) bands of the longitudinal and transverse modes of the silver nanorods, respectively. In fact, it was previously reported that the main SPR peaks for Ag nanorods and nanowires appear at ∼350 and ∼380 nm [44–51]. In some reports (e.g. [47, 48]), the peaks were attributed to the SPR bands of the longitudinal and transverse modes of Ag nanowires, respectively. However, in [49, 50], the same peaks were attributed to the out-of-plane quadrupole and out-of-plane dipole resonance modes (transverse modes) of the one-dimensional Ag structures, respectively. Figure 2 also shows a tail band above 450 nm, which can be attributed to the overlapping of the in-plane quadrupole and dipole resonance modes of the Ag nanowires with peaks at 445 and 514 nm, respectively [50].

Figure 3 shows the XRD spectrum of the silver nanorods grown on the Ti layer. The peaks were assigned to diffraction from the (111), (200) and (220) planes of metallic silver with a face-centered cubic (fcc) structure. A peak related to metallic Ti with (200) orientation was also observed very near the Ag(111) peak. The lattice constant of the silver nanorods was calculated as 0.4089 nm, which shows good consistency with the value of 0.4086 nm in the literature [52]. The intensity
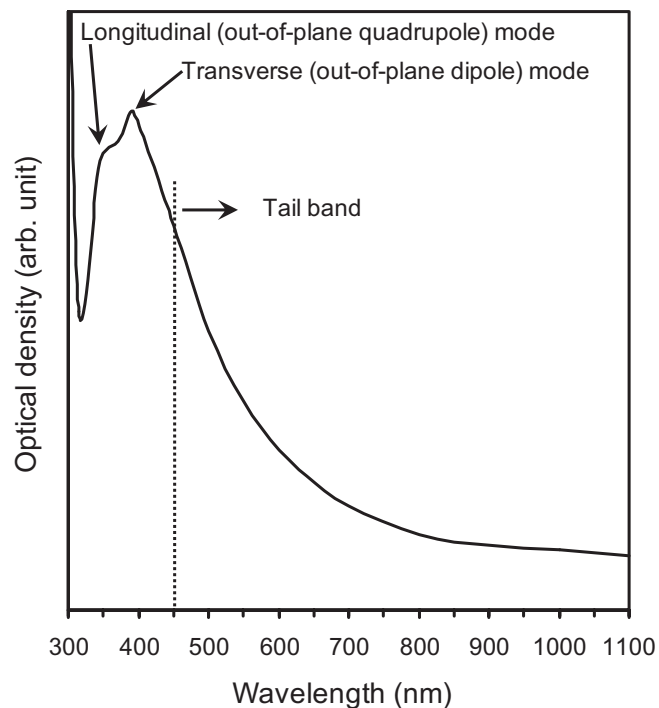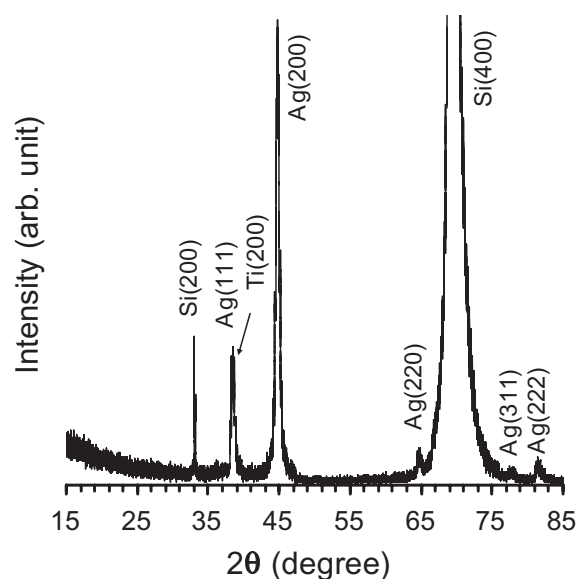

Figure 3. XRD spectrum of silver nanorods grown on a Ti interlayer.

ratios of (200)/(111) and (220)/(111) peaks were measured as 3.43 and 0.25, respectively, indicating the abundance of {100} facets, as also shown in the growth mechanism of silver nanorods and nanowires [45]. The mean crystallite size (D) of the silver nanorods was determined as 20 nm using the Scherrer method for the (200) diffraction peak, consistent with the SEM observation.

The antibacterial property of the grown Ag nanorods against *E. coli* bacteria was investigated at various applied electric fields. Figure 4 shows the results obtained. It can be seen that the number of viable bacteria reduced exponentially.
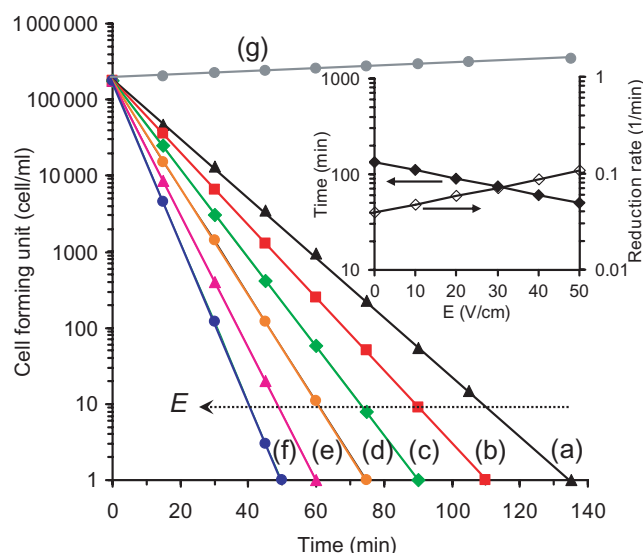
3

Figure 4. Number of colony forming units of *E. coli* cultured for various periods in the medium containing silver nanorods grown on a Ti interlayer at various values of the applied electric field *E*: (a) 0, (b) 10, (c) 20, (d) 30, (e) 40 and (f) 50 V cm^{-1} compared with a blank (control) sample (g). The inset shows the variation of the time required to kill all the bacteria and also the relative rate of reduction of the number of viable bacteria in terms of the applied electric field.

The slope of the fitted line yields the relative rate of reduction of the number of viable bacteria. Without applying an electric field to the silver nanorods, the rate of reduction of the number of viable bacteria was calculated as 3.9×10^{-2} min^{-1}, corresponding to a time of 135 min to kill all the bacteria (10^5 cfu ml^{-1}) under our experimental conditions. It was previously observed (not shown here) that 11 h was required for the complete removal of all bacteria in the presence of thin films containing cubic silver nanoparticles (shown in figure 1(a)). By applying an electric field, the antibacterial activity of the silver nanorods was promoted. Increasing the applied electric field from 10 to 50 V cm^{-1} enhanced the rate of reduction of the number of viable bacteria from 4.8×10^{-2} to 10.5×10^{-2} min^{-1}. This increase corresponds to a 63% reduction in the time required to kill all the bacteria from 110 to 50 min. However, for the cubic silver nanoparticles (figure 1(a)), after applying an electric field of 50 V cm^{-1}, the reduction in the time was less than 1 h, i.e. less than 10%. Therefore, the surface topography of the grown silver nanostructures is a significant parameter determining the antibacterial activity of the films. The inset of figure 4 shows that the application of an electric field leads to an exponential reduction in the time required to kill all the bacteria and correspondingly to an exponential increase in the rate of reduction of the number of viable bacteria in the solution. Increasing the applied electric field corresponds to increasing the silver ion concentration near the tips of the silver nanorods and /or in the solution without any change in the linear trend observed in the range 0–50 V cm^{-1}. Therefore, an increase in the applied electric field should result in the same exponential reduction in the time required to kill all the bacteria. The fitted line in the inset of figure 4 satisfies the equation $t = 135 \times 10^{-E/115}$, where t is the time required to kill all the

bacteria in min and E is the applied electric field in V cm^{-1}. This equation shows that the effective electric field (defined as the electric field required for a 90% reduction in t at $E = 0$) is 115 V cm^{-1} under our experimental conditions.

The antibacterial activity of silver ions on microorganisms is a well-known effect, but the bactericidal mechanism is only partially understood. It has been proposed that silver ions interact with the thiol groups of proteins, which are important for bacterial respiration and the transport of substances through the cell wall [53, 54]. In addition, silver ions can bind to the bacterial cell wall and thus alter the function of the bacterial cell membrane [24, 25]. Experimental evidence also suggests that the interaction of silver ions with bacteria causes their DNA molecules to lose their replication capability [24]. However, silver metal is slowly changed to silver ions in physiological systems and also in environments containing microorganisms at, for example, room temperature. By applying an electric field in the direction of grown silver nanorods, the free positive charges of the metallic silver nanorods become highly concentrated on their tips. This means that by applying an electric field, more silver ions are available on the tip surface to interact with bacteria. In addition, the nonuniform and strong electric field produced near the tips of the nanorods attracts the bacteria to the tips, increasing the probability that they come in contact with silver ions. Our proposed method may be useful for medical applications and the food-packaging and -preserving industries, where strong and fast antibacterial action is required at low temperatures (e.g. human body or room temperature).

4. Conclusions

Bactericidal silver nanorods with a polygonal cross section, a width of 20–60 nm, a length of 260–550 nm and a tip aspect ratio of 0.4–0.7 were successfully grown and aligned on a titanium interlayer by applying an electric field perpendicular to the surface of a Ag/Ti/Si(100) thin film during its heat treatment at 700 °C in an Ar + H$_2$ environment. The optical absorption spectrum of the silver nanorods displayed the corresponding SPR bands at wavelengths of 350 and 395 nm, corresponding to the longitudinal (out-of-plane quadrupole) and transverse (out-of-plane dipole) modes of the one-dimensional silver nanostructures, respectively. XRD analysis showed that crystallized silver nanorods with an fcc structure and a crystal size of about 20 nm were abundant in {100} facets. It was found that the grown silver nanorods show strong and fast antibacterial activity against *E. coli* bacteria. Applying an electric field in the direction of the nanorods (without any electrical connection between the nanorods and the capacitor plates producing the electric field) promoted their antibacterial activity, because it increased the silver ion concentration on the tips of the nanorods and also attracted the bacteria toward the silver nanostructures. It was shown that in the absence of an electric field, the rate of reduction of the number of viable bacteria was 3.9×10^{-2} min^{-1}, corresponding to a time of 135 min to kill all the bacteria. However, by increasing the electric field from 10

to $50 \, \text{V cm}^{-1}$, the rate of reduction exponentially increased from 4.8×10^{-2} to $10.5 \times 10^{-2} \, \text{min}^{-1}$, corresponding to a reduction of the time required for the complete removal of the bacteria from 110 to 50 min. Therefore, aligned silver nanorods on a Ti layer with an electric field can be utilized in the medical and food-preserving industries, which require an efficient antibacterial material that is effective at low temperatures.

Acknowledgments

References

[1] Geckeler K E and Rosenberg E (ed) 2006 *Functional Nanomaterials* (Valencia, USA: American Scientific Publishers)
[2] Chen C-Y and Chiang C-L 2008 *Mater. Lett.* **62** 3607
[3] Nakamura H, Tanaka M, Shinohara S, Gotoh M and Karube I 2007 *Biosens. Bioelectron.* **22** 1920
[4] Beyth N, Yudovin-Farber I, Bahir R, Domb A J and Weiss E I 2006 *Biomaterials* **27** 3995
[5] Kostowskyj M A, Gilliam R J, Kirk D W and Thorpe S J 2008 *Int. J. Hydrog. Energy* **33** 5773
[6] Ni K, Chen L and Lu G 2008 *Electrochem. Commun.* **10** 1027
[7] Ramnani S P, Sabharwal S, Vinod Kumar J, Hari Prasad Reddy K, Rama Rao K S and Sai Prasad P S 2008 *Catal. Commun.* **9** 756
[8] Shashikala V, Siva Kumar V, Padmasri A H, David Raju B, Venkata Mohan S, Nageswara Sarma P and Rama Rao K S 2007 *J. Mol. Catal. A: Chem.* **268** 95
[9] Feng J, Zhao X, Liu B and Zhou X 2008 *Opt. Commun.* **281** 5041
[10] Chu T C, Liu W-C and Tsai D P 2005 *Opt. Commun.* **246** 561
[11] Park K, Seo D and Lee J 2008 *Colloids Surf.* A **313–314** 351
[12] Alqudami A, Annapoorni S, Sen P and Rawat R S 2007 *Synth. Met.* **157** 53
[13] Jiang L, Wang W, Wu D, Zhan J, Wang Q, Wu Z and Jin R 2007 *Mater. Chem. Phys.* **104** 230
[14] Gibbard J 1937 *J. Am. Public Health* **27** 122
[15] Hill W R and Pillsbury D M 1939 *Argyria—The Pharmacology of Silver* (Baltimore, MD: Williams & Wilkins)
[16] Berger T J, Spadaro J A, Chapin S E and Becker R O 1976 *Antimicrob. Agents Chemother.* **9** 357
[17] Toshikazu T 1999 *Inorg. Mater.* **6** 505
[18] Burrell R E, Heggers J P, Davis G J and Wright J B 1999 *Wounds* **11** 64
[19] Thomas S and McCubbin P 2003 *J. Wound Care* **12** 101
[20] Tien D-C, Tseng K-H, Liao C-Y and Tsung T-T 2008 *Med. Eng. Phys.* **30** 948
[21] Vukcevic M, Kalijadis A, Dimitrijevic-Brankovic S, Lausevic Z and Lausevic M 2008 *Sci. Technol. Adv. Mater.* **9** 015006

[22] Kyriacou S V, Brownlow W J and Xu X H 2004 *Biochemistry* **43** 140
[23] Yuranova T, Rincon A G, Bozzi A and Parra S 2003 *J. Photochem. Photobiol.* A **161** 27
[24] Feng Q L, Wu J, Chen G Q, Cui F Z, Kim T N and Kim J O 2000 *J. Biomed. Mater. Res.* **52** 662
[25] Percival S L, Bowler P G and Russell D 2005 *J. Hosp. Infect.* **60** 1
[26] Thati B, Noble A, Rowan R, Creaven B S, Walsh M, McCann M, Egan D and Kavanagh K 2007 *Toxicol. In Vitro* **21** 801
[27] Betbeze C M, Wu C C, Krohne S G and Stiles J 2006 *Am. J. Vet. Res.* **67** 1788
[28] Dowsett C 2004 *Nurs. Stand.* **19** 56
[29] Norrby S R, Nord C E and Finch R 2005 *Lancet Infect. Dis.* **5** 115
[30] Tenover F C 2005 *Clin. Microbiol. Newsl.* **27** 35
[31] Ichinose N, Ozaki Y and Kashu S 1992 *Superfine Particle Technology* (New York: Springer)
[32] Lee H J, Yeo S Y and Jeong S H 2003 *J. Mater. Sci.* **38** 2199
[33] Lok C N, Ho C M, Chen R, He Q Y, Yu W Y, Sun H, Tam P K H, Chiu J F and Che C M 2006 *J. Proteome Res.* **5** 916
[34] Morones J R, Elechiguerra J L, Camacho A, Holt K, Kouri J B, Ramirez J T and Yacaman M J 2005 *Nanotechnology* **16** 2346
[35] Maneerung T, Tokura S and Rujiravanit R 2008 *Carbohydr. Polym.* **72** 43
[36] Mahapatra S S and Karak N 2008 *Mater. Chem. Phys.* **112** 1114
[37] Xu K, Wang J-X, Kang X-L and Chen J-F 2009 *Mater. Lett.* **63** 31
[38] Davis C P, Wagel N, Anderson M D and Warren M M 1993 *J. Urol.* **150** 1172
[39] Spadaro J A, Berger T J, Barranco S D, Chapin S E and Becker R O 1974 *Antimicrob. Agents Chemother.* **6** 637
[40] Spadaro J A 1981 *IEEE Trans. Biomed. Eng.* **28** 588
[41] Betts A J, Dowling D P, McConnell M L and Pope C 2005 *Mater. Des.* **26** 217
[42] Akhavan O and Moshfegh A Z 2007 *Appl. Surf. Sci.* **254** 548
[43] Agrawal V V, Kulkarni G U and Rao C N R 2008 *J. Colloid Interface Sci.* **318** 501
[44] Tsuji M, Nishizawa Y, Matsumoto K, Miyamae N, Tsuji T and Zhang X 2007 *Colloids Surf.* A **293** 185
[45] Tsuji M, Matsumoto K, Jiang P, Matsuo R, Tang X-L and Kamarudin K S N 2008 *Colloids Surf.* A **316** 266
[46] Tsuji M, Matsumoto K, Miyamae N, Tsuji T and Zhang X 2007 *Cryst. Growth Des.* **7** 311
[47] Sun Y G, Gates B, Mayers B and Xia Y N 2002 *Nano Lett.* **2** 165
[48] Sun Y G, Mayers B, Herricks T and Xia Y N 2003 *Nano Lett.* **3** 955
[49] Gao Y *et al* 2005 *J. Phys. D: Appl. Phys.* **38** 1061
[50] Gao Y *et al* 2005 *J. Cryst. Growth* **276** 606
[51] Gao Y *et al* 2006 *J. Cryst. Growth* **289** 376
[52] X-ray powder diffraction file, JCPDS-ICDD *Joint Committee on Powder Diffraction Standard-International Centre for Diffraction Data* Swarthmore, PA (a) 04–0783
[53] Cho K H, Park J E, Osaka T and Park S G 2005 *Electrochim. Acta* **51** 956
[54] Ivan S and Branka S S 2004 *J. Colloid Interface Sci.* **275** 177